Supporting Information

Lyssiotis et al. 10.1073/pnas.0903860106

SI Text

A structure and activity relationship analysis of a 100-member paullone collection (1, 2) in the NL assay demonstrated that the core paullone scaffold is sensitive to modification and that kenpaullone is the most active member (Fig. S5 and Table S1). Interestingly, however, various analogs that have no kinase-inhibiting activity against canonical kenpaullone kinase targets (i.e., CDK1, CDK5, GSK-3β) were still active in the Nanog reporter assay (Fig. S5). One analog (Kun152) that was active in the Nanog assay (2.4-fold relative to DMSO-treated controls) but ineffectual toward the canonical paullone kinases (>10 μM) and did not activate Wnt signaling (Fig. S5*F*) was selected for further kinase profiling. Kun152 demonstrated negligible activity against a 57-member tyrosine kinase profile at 5 μM in vitro (Table S2), indicating that it is not a nonselective kinase inhibitor. Collectively these data, together with the data shown in Fig. 3*F* and Fig. S4, suggest that the Nanog-activating ability of the paullone scaffold does not result from inhibition of the canonical kinase targets or from general inhibition of tyrosine kinase(s).

SI Materials and Methods

Characterization of Kenpaullone (3). 9-Bromo-7,12-dihydro-indolo[3,2-*d*][1]benzazepin-6(*5H*)-one, $C_{16}H_{11}BrN_2O$. The purity of each purchased compound was checked by NMR and MS. ^{1}H NMR (400MHz, DMSO-d_6): δ = 11.81 (*br*.s, 1H, NH), 10.13 (*br*.s, 1H, NH), 7.92 (d, J = 2.0 Hz, 1H), 7.73 (dd, J = 8.2, 1.4 Hz, 1H), 7.42–7.37 (m, 2H), 7.32–7.24 (m, 3H), 3.35 (s, 2H). ^{13}C NMR (100MHz, DMSO-d_6): δ = 171.4, 136.0, 135.6, 134.0, 128.5, 128.4, 128.3, 127.0, 124.5, 123.7, 122.3, 120.4, 113.4, 111.7, 107.2, 31.3. MS (EI), *m*/*z*: 327, 328, 329, 349, 351.

Chemicals. Synthesis of the 100-member paullone collection was described previously (2, 4, 5). All CDK and GSK-3β inhibitors were purchased from Calbiochem except for kenpaullone and purvalanol A, purchased from Sigma, and CHIR99021, purchased from Axon MedChem.

Gene Targeting and Blastocyst Injection. The NL targeting vector was generated by first subcloning a PGK-neomycin cassette flanked by 2 loxP sites into a pSP72 vector with BamHI and XhoI. The 5′ targeting arm was inserted into this BamHI site and a ClaI site in the pSP72 vector. The 5′ arm spanned 1,188 bp of the *Nanog* promoter and was flanked by a ClaI site at the 5′ end and a BamHI site at the 3′ end. These restriction sites were added to the PCR primers that were used to amplify the 5′ arm from a BAC containing this region of the *Nanog* promoter. The primers for PCR of the 5′ arm were as follows: forward, ATCGATCTGGGTTAGAGTGTCTTTCACTCAC; reverse, GGATCCGTCAGTGTGATGGCGAGGGAAGGG. The 3′ arm spanned 1.4 kb of *Nanog* intron 2 and was amplified from a BAC using the following PCR primers: forward, GCGGCCGCGTAAGGAATTCAGTCCCCGAA, reverse, GCGGCCGCCTCGAGGCCCTCTTCTGGAGTGTCTGAAGAC. The 3′ arm was cloned into the XhoI site of the vector. A 1.9-kb NcoI/BamHI fragment of pGL3-basic (Promega) containing the firefly luciferase gene and a SV40 pA signal was blunt-end–ligated into the vector.

For targeting, the NL vector was linearized with XhoI and electroporated into ES cells. G418 selection (350 μg/mL) was started 24 h after electroporation and continued for 10–12 days. Resistant clones were selected and expanded for screening by Southern blot analysis. DNA from resistant clones was digested with PvuII and run on a 0.8% agarose gel. The 3′ end homologous recombination was examined by a 415-bp external probe that was PCR-amplified from *Nanog* intron 2 using the following primers: forward, GCTACCTGAGACCCTATCCCTTAG; reverse, CATCTCACCAGCCCTACATACAGTG. This 3′ external probe identified the *Nanog* wild-type allele 6.4-kb PvuII fragment and the NL-targeted allele 4.7-kb PvuII fragment. The 5′ end homologous recombination of resistant clones was analyzed using a 340-bp XbaI/HindIII fragment of the NL targeting vector. This internal probe identified a wild-type 6.4-kb PvuII fragment and a targeted 5.2-kb PvuII fragment (Fig. 1*B*).

Cell Culture and Viral Infections. O4N-MEFs (at passage 1–2; 5×10^4 cells/well of a 6-well dish) were infected overnight with concentrated viral supernatant. Virus was generated by transfection (FugeneHD; Roche) of GP2–293 packaging cells (Clontech) with Moloney-based retroviral vector pMXs containing the cDNA of Oct4, Sox2, and c-Myc with or without Klf4 (Addgene, deposited by S. Yamanaka) together with the VSV-G packaging plasmid. Media and compound (or vehicle control, DMSO 0.05%) were changed every 2–3 days. At day 20, selection was initiated by adding G418 (300 μg/mL) to the culture media. Colonies were counted (based on survival) or passaged onto irradiated MEFs in ES cell growth media at day 25.

O4G-MEFs (at passage 1–2; 10^4 cells/well of a 6-well dish) were infected with pooled viral supernatant generated by transfection of HEK293T cells (Fugene; Roche) with doxycycline-inducible lentiviral vectors (6) containing the cDNAs of Oct4, Sox2, and c-Myc with or without Klf4, together with a plasmid encoding the VSV-G envelope protein. The medium was supplemented the next day with doxycycline (2 μg/mL) and kenpaullone or DMSO. Green colonies were selected 2 weeks later and expanded under ES cell growth conditions.

NPCs (at passage 4–5; 10^5 cells/well of a 6-well dish) were infected overnight with concentrated viral supernatant generated with the following plasmids: pMXs-Oct4 with or without pMXs-Klf4 and pCIGAR-Myc (a murine stem cell virus–based bicistronic retroviral vector modified to permit Gateway-mediated insertional recombination of full-length or ORF transgenes immediately upstream of an IRES-eGFP marker). Compounds were added 12 h later and changed every 2 days thereafter. At day 8, colonies were either fixed and stained for AP or passaged onto irradiated MEFs in ES cell growth media.

Colony-forming assays with secondary OSM-MEFs were performed as described previously (7) and analyzed for Oct4 expression 25 days later.

Chemical Screening and Nanog Assay. NL-MEFs ($\approx 10^8$ cells) were transduced at passage 1 with concentrated VSV-G–pseudotyped Oct4-, Sox2-, and c-Myc–expressing lentivirus in 15-cm dishes. Immunofluorescence staining confirmed that >90% of NL-MEFs expressed Oct4 (polyclonal mouse; Santa Cruz Biotechnology) and Sox2 (monoclonal mouse; Santa Cruz Biotechnology). OSM-transduced NL-MEFs were expanded 4 passages $\approx$2 weeks before screening. For large-scale screens, the OSM NL-MEFs were plated into 1,536-well plates at 500 cells/well in mouse ES cell growth media supplemented with LIF (20 ng/mL). Compounds were added at a final concentration of 2.2 μM (20 nL of 1 mM stock solutions in 9 μL of media) immediately after plating. Nanog-driven luciferase expression was assayed 10 days later by adding 2 μL of Bright-Glo reagent (Promega). Primary hits were rescreened in triplicate in a 1,536-well format. Dose–

response curves were generated by screening OSM NL-MEFs in an 8-part dilution (1 mM stock, half-log serial dilutions) in a 384-well format. Jackknife z-score values, the 1-sample Kolgomorov-Smirnov test value ($P = .54$), and the empirical and theoretical inverse-gamma distribution were calculated according to Malo et al. (8) and references therein.

An HEK293T counterscreening cell line was generated by cotransfecting the pGL3 SV40-luciferase vector (E1761; Promega) with pcDNA3.1+ (V790–20; Invitrogen) encoding the gene for neomycin resistance. Neomycin selections (400 μg/mL) were carried out for 7 days. The SV40-luciferase HEK293T line was passaged in DMEM plus 10% FBS. Hits that reconfirmed in triplicate in NL-MEFs were screened in SV40-luc 293T cells to filter out false-positives (9).

Counterscreening, dose–response experiments, structure and activity relationship analysis, and time course experiments were run in 384-well plates (Greiner). Cells were plated at 1,000 cells/well in ES cell growth media and assayed 10 days later unless specified otherwise. All luciferase readings were acquired after the addition of Bright-Glo reagent (Promega). All experiments were run in duplicate and repeated at least 3 times.

Time Course Analysis. OSM-transduced NL-MEFs were plated at 1,000 cells/well in ES cell growth media, treated with kenpaullone (5 μM), and assayed at the indicated time points. All luciferase readings were acquired after the addition of Bright-Glo reagent (Promega). The cell number was normalized at each time point by assaying parallel plates for total ATP levels using Cell Titer-Glo reagent (Promega). The assay was run in 384-well plates (Greiner).

Quantitative and Semiquantitative RT-PCR. Total RNA was obtained and reverse-transcribed, as described previously (10). TaqMan real-time PCR was performed using TaqMan Gene Expression Master Mix (Applied Biosystems) and an ABI Prism 7900HT fast real-time PCR system with Klf4 probes (Applied Biosystems; Mm 00516105_g1, MGB probe) and normalized to GAPDH (4326317E, VIC probe) as endogenous controls.

For semiquantitative analyses, PCR was performed using the Phusion polymerase (New England Biosciences) and gene-specific primers (Table S4). Cycle parameters were 10 s at 98 °C; 15 s at 51 °C (CDK1), 54 °C (CDK2), 63 °C (GSK-3β), 61 °C (CDK5), or 67 °C (Nat1); and 30 s at 72 °C for 30 cycles. The total RNA and PCR conditions were optimized so that amplification of both *Nat1* and the cDNAs of interest were in the exponential phase.

Western Blot Analysis. Protein extraction, preparation, gel electrophoresis, and transfer were performed as described previously (11). Membranes were blocked (with 5% nonfat dry milk in Tris-buffered saline with 0.5% Tween-20), washed, and incubated with primary antibodies [Klf4 (Santa Cruz Biotechnology); γ-tubulin (Sigma); β-actin) in the blocking solution for 2 h at room temperature or 4 °C overnight. They were then washed and incubated with the corresponding horseradish peroxidase–conjugated secondary antibodies at room temperature for 1 h. Finally, membranes were washed and subjected to enhanced chemiluminescence detection.

Short-Hairpin Knockdowns. Lentiviral particles containing shRNAs were generated by transfecting HEK293T cells (FugeneHD; Roche) with pooled pLL3.7 vectors encoding the desired knockdown (Table S4), packaging vectors, and VSV-G. Then 72 h later, viral supernatant was collected, concentrated (Amicon), and applied to OSM-transduced NL-MEFs. Individual cell lines were created for each kinase knockdown. Two days later, the cells were sorted for pLL3.7-driven GFP; flow cytometric analysis indicated infectivity of >90%. Combinatorial knockdown was achieved by treating single knockdown lines with lentiviral particles targeting additional kinases.

O4N-MEFs at passage 1–2 were infected with pooled viral supernatant containing shRNAs targeting CDK1, CDK2, CDK5, and GSK-3β. Two weeks later, the cells were fixed and AP-stained.

1. Leost M, et al. (2000) Paullones are potent inhibitors of glycogen synthase kinase-3beta and cyclin-dependent kinase 5/p25. *Eur J Biochem* 267:5983–5994.
2. Schultz C, et al. (1999) Paullones, a series of cyclin-dependent kinase inhibitors: Synthesis, evaluation of CDK1/cyclin B inhibition, and in vitro antitumor activity. *J Med Chem* 42:2909–2919.
3. Kunick C (1992) Synthese von 7,12-Dihydro-indolo[3,2-d][1]benzazepin-6-(5H)-onenund 6,11-Dihydro-thieno-[3′,2′:2,3]azepino[4,5-b]indol-5(4H)-on. *Arch Pharm* 325:297–299.
4. Kunick C, Lauenroth K, Leost M, Meijer L, Lemcke T (2004) 1-Azakenpaullone is a selective inhibitor of glycogen synthase kinase-3 beta. *Bioorg Med Chem Lett* 14:413–416.
5. Kunick C, et al. (2005) Structure-aided optimization of kinase inhibitors derived from alsterpaullone. *Chembiochem* 6:541–549.
6. Brambrink T, et al. (2008) Sequential expression of pluripotency markers during direct reprogramming of mouse somatic cells. *Cell Stem Cell* 2:151–159.
7. Markoulaki S, et al. (2009) Transgenic mice with defined combinations of drug-inducible reprogramming factors. *Nat Biotechnol* 27:169–171.
8. Malo N, Hanley JA, Cerquozzi S, Pelletier J, Nadon R (2006) Statistical practice in high-throughput screening data analysis. *Nat Biotechnol* 24:167–175.
9. Auld DS, Thorne N, Maguire WF, Inglese J (2009) Mechanism of PTC124 activity in cell-based luciferase assays of nonsense codon suppression. *Proc Natl Acad Sci USA* 106:3585–3590.
10. Lyssiotis CA, et al. (2007) Inhibition of histone deacetylase activity induces developmental plasticity in oligodendrocyte precursor cells. *Proc Natl Acad Sci USA* 104:14982–14987.
11. Zhu S, et al. (2009) A small molecule primes embryonic stem cells for differentiation. *Cell Stem Cell* 4:416–426.
12. Liu J, et al. (2005) A small-molecule agonist of the Wnt signaling pathway. *Angew Chem Int Ed Engl* 44:1987–1990.
13. Knockaert M, et al. (2002) Intracellular targets of paullones: Identification following affinity purification on immobilized inhibitor. *J Biol Chem* 277:25493–25501.
14. Zaharevitz DW, et al. (1999) Discovery and initial characterization of the paullones, a novel class of small-molecule inhibitors of cyclin-dependent kinases. *Cancer Res* 59:2566–2569.
15. Meijer L, Flajolet M, Greengard P (2004) Pharmacological inhibitors of glycogen synthase kinase 3. *Trends Pharmacol Sci* 25:471–480.
16. Mettey Y, et al. (2003) Aloisines, a new family of CDK/GSK-3 inhibitors: SAR study, crystal structure in complex with CDK2, enzyme selectivity, and cellular effects. *J Med Chem* 46:222–236.
17. Meijer L, et al. (2003) GSK-3–selective inhibitors derived from Tyrian purple indirubins. *Chem Biol* 10:1255–1266.
18. Wan Y, et al. (2004) Synthesis and target identification of hymenialdisine analogs. *Chem Biol* 11:247–259.
19. Gray NS, et al. (1998) Exploiting chemical libraries, structure, and genomics in the search for kinase inhibitors. *Science* 281:533–538.
20. Meijer L, et al. (1997) Biochemical and cellular effects of roscovitine, a potent and selective inhibitor of the cyclin-dependent kinases cdc2, cdk2, and cdk5. *Eur J Biochem* 243:527–536.
21. Davies TG, et al. (2002) Structure-based design of a potent purine-based cyclin-dependent kinase inhibitor. *Nat Struct Biol* 9:745–749.
22. Bhat R, et al. (2003) Structural insights and biological effects of glycogen synthase kinase 3–specific inhibitor AR-A014418. *J Biol Chem* 278:45937–45945.
23. Ring DB, et al. (2003) Selective glycogen synthase kinase 3 inhibitors potentiate insulin activation of glucose transport and utilization in vitro and in vivo. *Diabetes* 52:588–595.

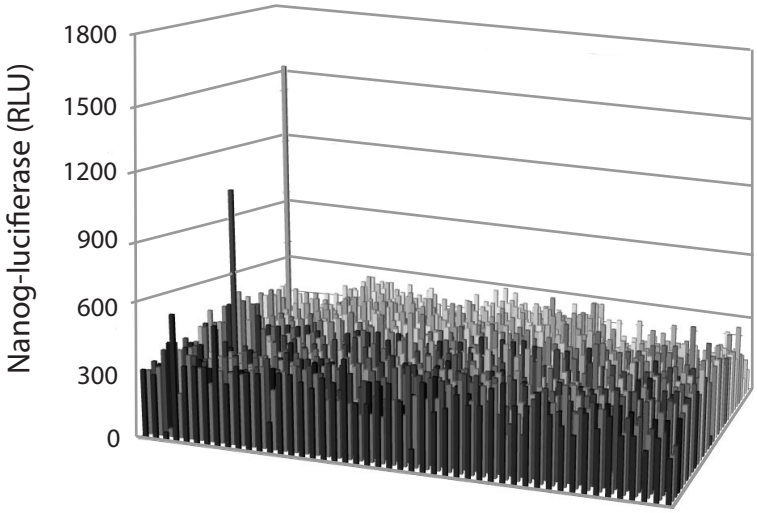

Fig. S1. NL validation assay. OSM-transduced NL-MEFs were treated with a known drug compound plate in a 1,536-well format and analyzed 10 days later for luciferase activity; values represent the mean of 3 independent runs. Nanog activity is reported in RLUs.

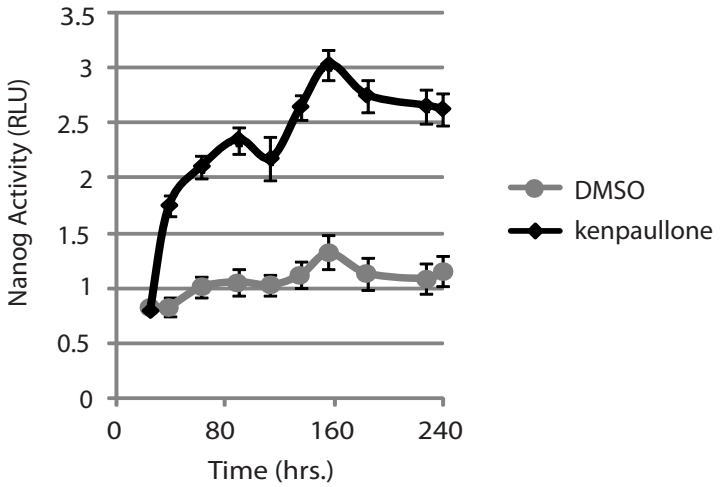

Fig. S2. Time course of Nanog activation. OSM-transduced NL-MEFs were treated with kenpaullone (5 μM) or DMSO (0.05%) and analyzed for luciferase activity as a function of time. Nanog expression is reported in RLUs and is normalized for cell number (obtained bt analysis of ATP concentration; read in parallel plates). Error bars indicate SD ($n = 3$).

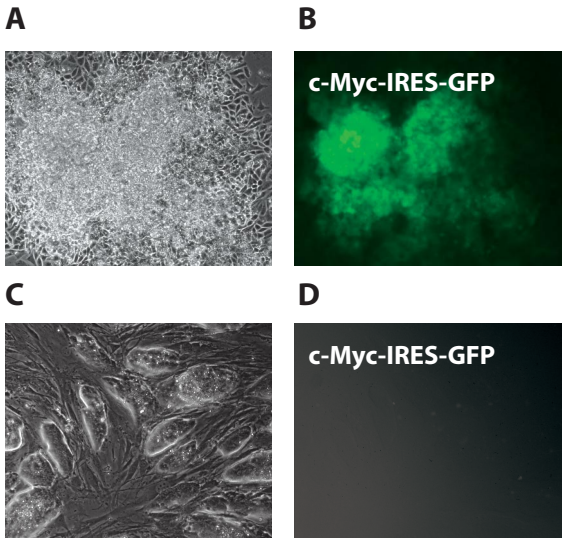

Fig. S3. Retroviral vectors are silenced in iPS cells derived from NPCs with Oct4/c-Myc and kenpaullone. NPCs were transduced with Oct4 and a c-Myc vector harboring an IRES-GFP cassette. After 8 days of kenpaullone treatment (5 μM) (*A*), definitive colonies expressing GFP were visible (*B*). Colonies passaged under mouse ES cell conditions resembled murine ES cells morphologically (*C*) and did not express GFP (*D*), consistent with the silencing of retroviral elements observed in reprogrammed cells.

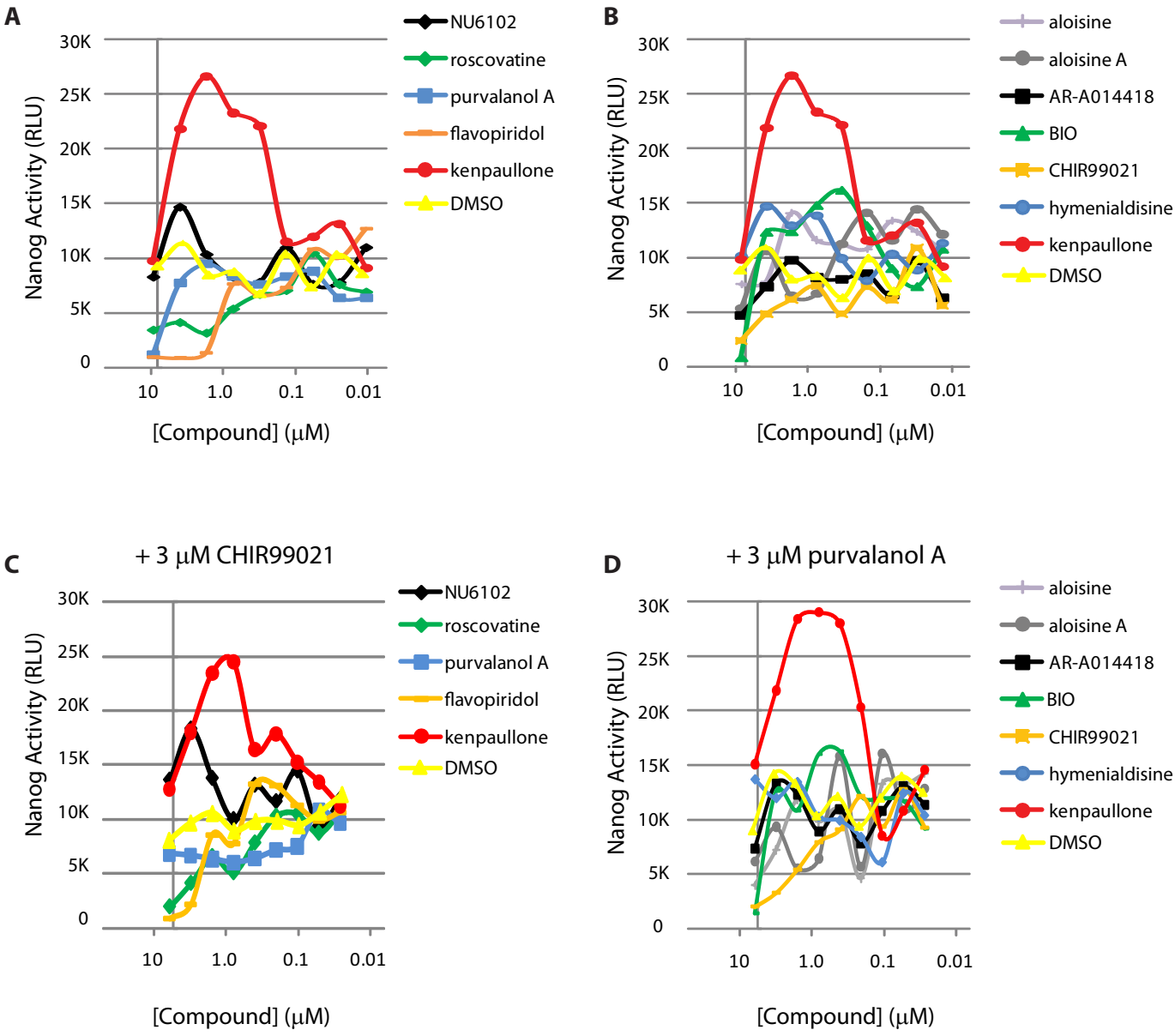

Fig. S4. Dual inhibition of CDKs and GSK-3β fails to recapitulate the activity of kenpaullone. OSM-transduced NL-MEFs were treated in a dose-dependent fashion with CDK (*A*) or GSK-3β inhibitors (*B*) in a 384-well format and analyzed for luciferase activity 10 days later. OSM-transduced NL-MEFs were plated in screening media containing a potent selective GSK-3β inhibitor (CHIR99021, 3 μM) (*C*) or a general CDK inhibitor (purvalanol A, 3 μM) (*D*) and treated in a dose-dependent manner with CDK or GSK-3β inhibitors, respectively. Ten days after treatment, the cells were analyzed for luciferase expression. Data points represent the mean of triplicate runs and are representative of at least 3 independent experiments. Values that drop off sharply at high concentration indicate cellular toxicity. Kinase inhibition data are presented in Table S3.

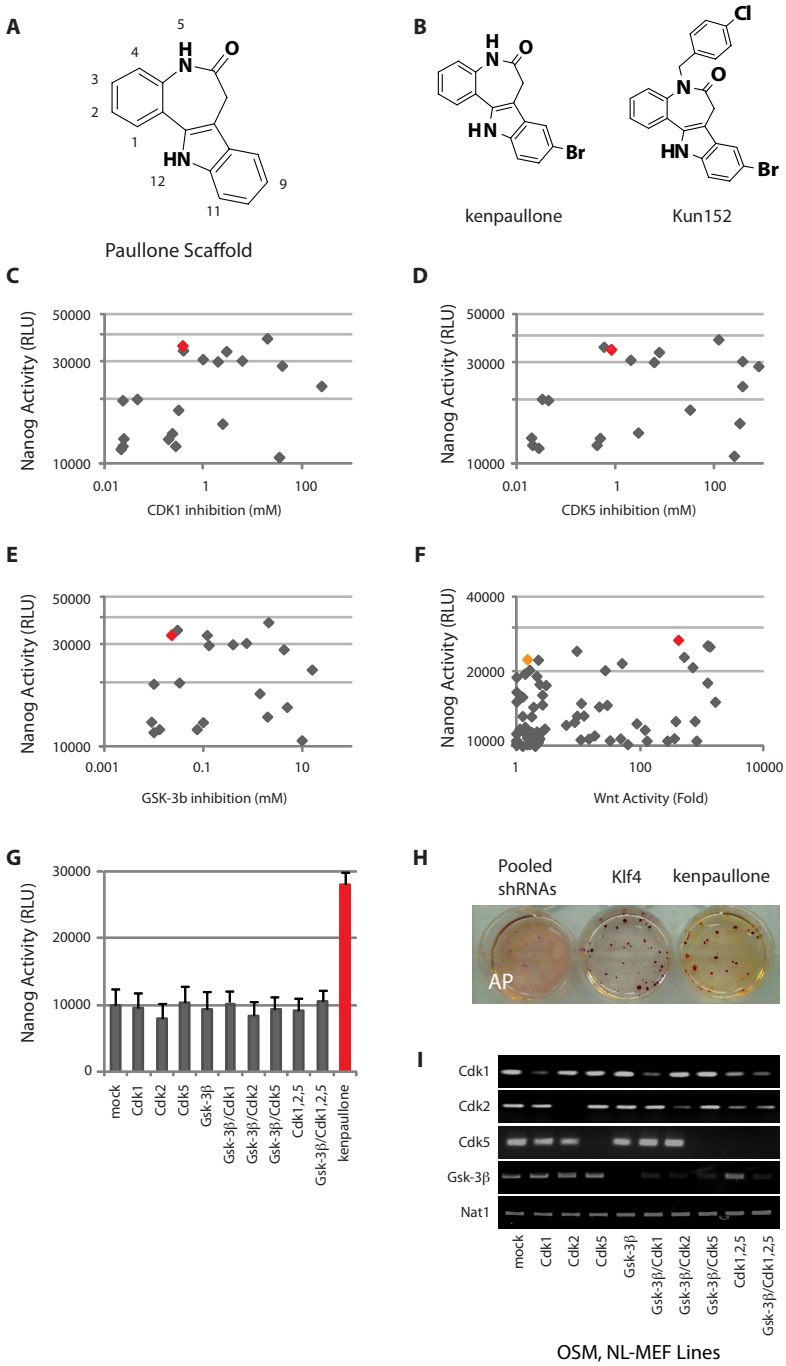

Fig. S5. Paullone-induced activation of Nanog activity does not result from inhibition of the canonical paullone kinase targets. (*A*) Paullone scaffold. Atom labeling corresponds to the structure and activity relationship analysis data given in Table S1. (*B*) Structure of kenpaullone and the paullone analog, Kun152, profiled for kinase activity. Kinase inhibition data are detailed in Table S2. (*C*–*E*) Plots of Nanog activity versus inhibition of CDK1 (*C*), CDK5 (*D*), or GSK-3β (*E*). Each point on the graph represents a different member of the paullone collection. Kenpaullone is depicted in red. Kinase inhibition data, obtained previously (1), and are plotted as the IC50 value in μM. (*F*) Nanog activity plotted against TCF/LEF-driven luciferase activity [representative of GSK-3β inhibition (12)] for the 100-member paullone library. Kun152 is depicted in orange. (*G*) OSM-transduced NL-MEFs were treated with lentiviral particles containing shRNAs targeting the canonical paullone kinase targets, either individually or in combination, and analyzed for luciferase expression 10 days later. Kenpaullone (5 μM) was included as a positive control. (*H*) Lentiviral particles containing shRNAs targeting CDK1, CDK2, CDK5, and GSK-3β were pooled and applied to OSM-MEFs. Cells were AP-stained 2 weeks later. Klf4 and kenpaullone (5 μM) were included as positive controls. (*I*) RT-PCR analysis of OSM-transduced NL-MEFs for the indicated knockdown(s). Data points presented in (*A*)–(*D*) represent the mean of triplicate runs and are representative of at least 3 independent experiments. Nanog and Wnt activity for the paullone analogs were plotted at the most active, nontoxic compound concentration. Error bars in (*G*) indicate SD (n = 5).

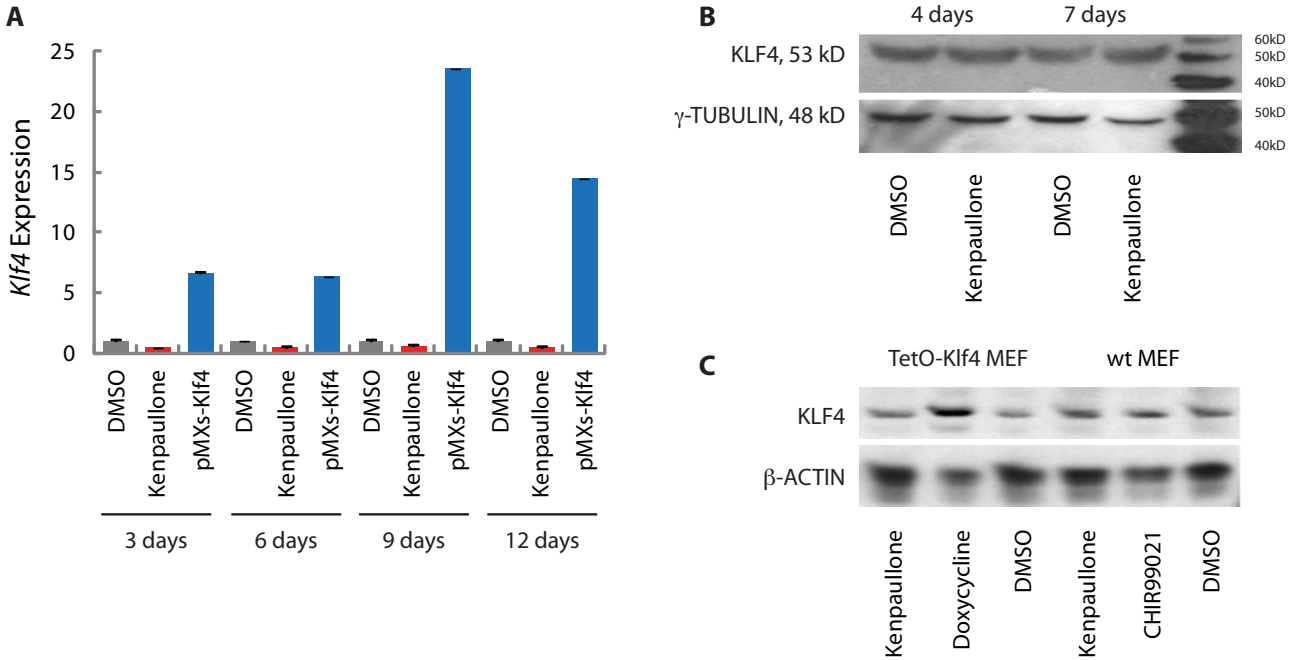

Fig. S6. Klf4 is not activated by kenpaullone. (*A*) OSM-transduced MEFs were treated with DMSO, retrovirally delivered Klf4, or kenpaullone (5 μM). Klf4 expression was analyzed at 3-day intervals by quantitative RT-PCR and normalized to GAPDH. Error bars indicate SD ($n = 3$). (*B*) Secondary MEFs carrying doxycycline-inducible proviruses encoding Oct4, Sox2, and c-Myc (7) were treated with kenpaullone (5 μM) or vehicle control and subjected to Western blot analysis for Klf4 expression at days 4 and 7. (*C*) Secondary MEFs carrying a doxycycline-inducible proviral copy of Klf4 (TetO-Klf4) were treated with kenpaullone (5 μM), vehicle control, or doxycycline (positive control). Wild-type MEFs were treated with kenpaullone (5 μM), a GSK-3β–specific inhibitor (CHIR99021, 3 μM), or vehicle control. Samples were analyzed by Western blot 92 h later. Data are representative of 3 independent experiments.

Table S1. Structure and activity relationship analysis of paullone SAR: Effects of substitution to the paullone scaffold (Fig. S5*A*) as determined by Nanog activity

Position	Substitution
1	C = N > S
2	H > OH > OCH_3 > short alkyl chain >>> bulky substituents (not tolerated)
2	C >> N (nitrogen abolishes activity)
3	H > OCH_3 > OH
4	H >> OH > OCH_3
4	C > N
5	H > CH_3 > hydroxy-amidine > p/Cl-Bz >> bulky substituents
9	Br = I = CH_3 > CF_3 > OCH_3 > Cl >>> bulky and (F,CN,OH,H,CO_2H, NO_2) not tolerated
11	C > N
12	N >> O
12	H > CH_3 >>> bulky substituents (not tolerated)

Data in bold represent modifications to the paullone carbon backbone.

Table S2. Tyrosine kinase panel

Kinase	% i
Abl	7
Abl (T315I)	12
Akt1	4
AMPK	10
AurB	15
AXL	11
BMX	−8
BTK	−7
CaMK2a	31
CDK2/cycA	19
CHK2	12
CK1a	5
cKit	−2
c-RAF	6
CSK	3
DYRK1a	4
EGFR	−2
EphA3	7
EphB3	2
FAK2	7
FGFR3	1
Flt3	15
FMS/CSF1R	31
Fyn	5
GSK3b	52
IGF1R	−12
IKKb	1
InsR	−29
IRAK4	1
JAK2	−1
JNK2a2	5
KDR	14
Lck	8
Lyn	23
MAPK1	3
MAPK13	−7
MAPK14	−6
MAPKAPK2	7
MET	5
NEK2	7
p70S6K	4
PAK2	1
PDGFRa	−6
PDK1	6
Pim2	3
PKA	−1
PKCa	−2
PLK1	6
RET	1
ROCK2	5
RSK1	3
SGK1	8
Src	11
Syk	1
TrkA	10
TTK	8
ZAP70	−14

Data are presented as percent kinase inhibition (% i) in the presence of 5 μM Kun 152. Kun152 increases the Nanog luciferase signal 2.4-fold relative to DMSO-treated controls.

Table S3. Kinase inhibition profile for the small-molecule inhibitors used in this study

Compound	Class	CDK1	CDK2/cyclin A	CDK2/cyclin E	CDK5	GSK-3β
Kenpaullone (13, 14)	Dual	0.4	0.68	7.5	0.85	0.23
Flavopiridol (15)	Dual	0.4	NA	NA	NA	0.45
Aloisine (16)	Dual	0.7	NA	NA	1.5	0.92
Aloisine A (16)	Dual	0.15	0.12	0.4	0.2	1.5
BIO (15, 17)	Dual	0.32	0.3	NA	3	0.005
Hymenialdisine (15, 18)	Dual	0.022	0.07	0.04	0.028	0.01
Purvalanol A (19)	CDKi	0.004	0.07	0.035	0.075	$>$10
Roscovatine (20)	CDKi	0.65	0.7	0.7	0.2	NA
NU6102 (21)	CDKi	0.01	0.0054	NA	NA	NA
AR-A014418 (15, 22)	GSKi	NA	$>$100	$>$100	$>$100	0.104
CHIR99021 (15, 23)	GSKi	8.8	NA	NA	NA	0.007

Class indicates whether the small molecule is a CDK inhibitor (CDKi), a GSK-3β inhibitor (GSKi), or an inhibitor of both CDKs and GSK-3β (dual). Data are reported as the IC50 in μM for in vitro kinase inhibition. NA, data not available.

Table S4. Forward and reverse primers used for semiquantitative RT-PCR and shRNA sequences used for knockdown analysis

Gene (NA #)	Nucleotide sequence
Nanog (NM_028016.2)	Forward: 5′-AGGGTCTGCTACTGAGATGCTCTG-3′
	Reverse: 5′-CAACCACTGGTTTTTCTGCCACCG-3′
Nat1 (NM_008673.1)	Forward: 5′- ATTCTTCGTTGTCAAGCCGCCAAAGTGGAG-3′
	Reverse: 5′-AGTTGTTTGCTGCGGAGTTGTCATCTCGTC-3′
Cdc2 (NM_007659)	Forward: 5′- GTCCGTCGTAACCTGTTGAG-3′
	Reverse: 5′-CATGTTAATTAAGTTATACGTAGG-3′
	Sh1: 5′-GCACCCGTACTTTGATGAC-3′
	Sh2: 5′-GGAGTGCCCAGTACTGCAA-3′
	Sh3: 5′-GGGACCATATTTGCAGAAC-3′
	Sh4: 5′-GAACACCTTTCCCAAGTGG-3′
Cdk2 (NM_183417)	Forward: 5′- GGAGAACTTTCAAAAGGTGG-3′
	Reverse: 5′-CCGTGAGAGCAGAGGCATCCATG-3′
	Sh1: 5′-GGGCCCTATTCCCTGGAGA-3′
	Sh2: 5′-GCCTGATTATAAGCCAAGT-3′
	Sh3: 5′-GCAGCCCTGGCTCACCCTT-3′
	Sh4: 5′-GCTGCTCCAGGGCCTGGCT-3′
	Sh5: 5′- GGTGTACCCAGTACTGCCA-3′
Gsk-3β (NM_019827.6)	Forward: 5′- CAGAGTCGCCAGACACTATAGTCGA-3′
	Reverse: 5′-GCCGGAAGACCTTTGTCCAA-3′
	Sh1: 5′-GTTCTACAGGACAAGCGAT-3′
	Sh2: 5′-GTGATTGGAAATGGATCAT-3′
	Sh3: 5′-GTTGTATATGTATCAGCTG-3′
	Sh4: 5′-GATGAGGTCTACCTTAACC-3′
	Sh5: 5′-GCATGAAAGTTAGCAGAGA-3′
Cdk5 (NM_007668.3)	Forward: 5′- TCTGAAGCGTGTCAGGCTGG-3′
	Reverse: 5′-ACAAGCTGTGGGCCACATCA-3′
	Sh1: 5′-GCTGCTGAAAGGCCTGGGA-3′
	Sh2: 5′-GGCTTCATGATGTCCTGCA-3′
	Sh3: 5′-GACTATAAGCCCTACCCAA-3′
	Sh4: 5′-GTGGTCAGCCGGCTGCATC-3′